A&A 474, 557–563 (2007)
DOI: 10.1051/0004-6361:20065840

Astronomy & Astrophysics

Modeling of RR Lyrae light curves: the case of M3⋆

M. Marconi[1] and S. Degl'Innocenti[2,3]

[1] INAF, Osservatorio Astronomico di Capodimonte, via Moiariello 16, 80131 Napoli, Italy
e-mail: marcella@na.astro.it
[2] Dipartimento di Fisica, Università di Pisa, Largo B. Pontecorvo 3, 56126 Pisa, Italy
[3] INFN, Sezione di Pisa, Largo B. Pontecorvo 3, 56126 Pisa, Italy

Received 15 June 2006 / Accepted 19 July 2007

ABSTRACT

Context. A promising technique to derive the physical parameters and the distance of pulsating stars is the fit of the observed light curves by nonlinear pulsation models.
Aims. We apply this technique to a subsample of the RR Lyrae belonging to the Galactic globular cluster M3. The application of the method to cluster pulsators has the advantage of dealing with a homogeneous sample at the same distance and with the same chemical composition allowing to be checked the internal consistency of pulsational calculations.
Methods. We selected seven pulsators (three RR_c and four RR_{ab}) which cover a significant period range and show detailed light curves in the B, V and in some cases I bands. For four of them, with different periods, pulsation modes and light curve properties, we analyze the dependence of the theoretical light curve variations on the model input parameters.
Results. For all selected objects, except the reddest one, we are able to theoretically reproduce the observed light curve morphology for self-consistent ranges of intrinsic stellar parameters, in agreement with the evolutionary predictions for the corresponding metal abundance. It is worth noting that, even if the theoretical reproduction of individual light curves gives for each variable only a range of stellar parameters and distances, the analysis of several variables belonging to the same cluster provides a mean distance modulus, namely $\mu_V = 15.10 \pm 0.1$ mag, and also checks the self-consistency of the adopted theoretical scenario. Taking also into account the evolutionary constraints, the range of the accepted distance modulus is significantly reduced giving a weighted mean value of 15.05 ± 0.02. Our estimates are in agreement with available results in the literature obtained from independent methods.

Key words. stars: evolution – stars: variables: RR Lyr – stars: distances

1. Introduction

During the last few decades many theoretical efforts have been devoted to the construction of nonlinear and convective pulsation codes for the modeling of classical helium burning pulsating stars, namely Cepheids and RR Lyrae (e.g. Gehmeyr 1992, 1993; Bono & Stellingwerf 1994 (BS94); Wood et al. 1997; Feuchtinger 1999 and references therein). One of the most important advantages of this kind of models is the unprecedented possibility to predict the time variations of the relevant stellar properties, such as luminosity, radius, effective temperature and surface gravity, along a pulsation cycle. On this basis one can attempt the reproduction of the observed light and radial velocity curves with those predicted by nonlinear pulsation models. This approach has the advantage of relying on the direct comparison between observed and predicted curves, rather than involving only related parameters such as pulsation amplitudes and Fourier parameters, performing the theoretical reproduction of both general features (period, shape, amplitude) and morphological details (bumps and dips), of the observed curves. Since the morphology of the curves depends on the model input parameters, as well as on the physical and numerical assumptions, the modeling of actual light and radial velocity variations along a pulsation cycle offers a unique opportunity to obtain sound estimates of the intrinsic stellar properties of the variables, providing at the same time a key test of current theoretical predictions.

The method has been successfully applied to both Classical Cepheids and RR Lyrae. Theoretical light curves for Cepheids were first presented by Wood et al. (1997, hereinafter WAS) for the LMC bump Cepheid HV905 and, more recently, by Bono et al. 2002 (BCM02) for two LMC fundamental mode Cepheids from the OGLE catalogue. An independent application to the MACHO V and R light curves of 20 bump Cepheids in the LMC (including HV905) was performed by Keller & Wood (2002), and more recently extended to a further 28 Magellanic objects (19 in the LMC and 9 in the SMC), on the basis of the same nonlinear pulsation code previously adopted by WAS (Keller & Wood 2006). The results obtained by BCM02 and Keller & Wood (2002, 2006) appear in good agreement, suggesting that the model fitting technique is not critically dependent on the adopted pulsation code, as well as on the physical and numerical assumptions in the model computations.

For RR Lyrae, the first attempt to compare the morphology of observed and predicted light curves was provided by Bono et al. (2000) (hereinafter BCM00). The authors modeled the multi-filter light curve (and the less accurate radial velocity curve) of the field first overtone pulsator U Com, obtaining a "pulsational" evaluation of the intrinsic stellar parameters and, in turn, of the distance of the variable. These results were found to be in good agreement with independent evaluations available in the literature, as well as with the predictions of stellar evolution theory. Similarly good results were later obtained by di Fabrizio et al. (2002) for another field RR_c pulsator, and by Castellani et al.(2002) for a fundamental mode RR pulsator

⋆ Figures 1–23 are only available in electronic form at http://www.aanda.org

Table 1. The range of estimated apparent visual distance modulus (μ_V), obtained with different methods, and the reddening values, $E(B-V)$, provided in the recent literature for M3. The [Fe/H] values given by Zinn & West (1984: ZW), Harris (2003: H) and Carretta & Gratton (1997: CG) are also reported.

Quantity	Value
μ_V	$14.8 \div 15.2$
$E(B-V)$	$0.01 \div 0.03$
$[Fe/H]_Z W$	-1.66 ± 0.06
$[Fe/H]_H$	-1.57
$[Fe/H]_C G$	-1.34 ± 0.06

in the galactic globular ω Cen. However, recently, Marconi & Clementini (2005, hereinafter MC05) by analyzing the B, V light curves of 14 RR Lyrae stars (7 fundamental and 7 first overtone pulsators) obtained an estimate of the distance modulus for the LMC in good agreement with distances derived from Cepheids, but with the evidence for a serious mismatch between observed and predicted light curves in the case of the longest period fundamental pulsators.

In this paper we rely on a suitable sample of RR Lyrae in a Galactic globular cluster. With this choice one has the advantage of dealing with an homogeneous sample of variables which are known to be all at the same distance and to have the same chemical composition, with intrinsic stellar parameters constrained by stellar evolution theoretical predictions. In particular, we choose the globular cluster (GC) M3, which is the Galactic cluster with the largest number of observed RR Lyrae variables (e.g. Clement et al. 2001; Corwin & Carney 2001, hereinafter CC01; Clementini et al. 2004), for which accurate multi-filter light curves are available (CC01, Hartman et al. 2005; Benkő et al. 2006).

RR Lyrae in M3 have been analyzed by several authors from the pulsational and evolutionary point of view. Here we quote the multicolor and Fourier study of a wide sample of RR Lyrae in M3 recently presented by Cacciari et al. (2005) and the analysis by Marconi et al. (2003; see also Jurcsik et al. 2003), who discussed the good agreement between theoretical and observed pulsational properties, in particular for the instability strip topology and the period-amplitude relations.

Table 1 reports the ranges of current independent determinations of the distance modulus and the reddening (e.g. Buonanno et al. 1994; Ferraro et al. 1999; Rood et al. 1999) for this cluster. Metal abundance values provided by various authors are also reported. Here we adopt the [Fe/H] value of Carretta & Gratton (1997) and assume an enhancement of α elements $[\alpha/Fe] \approx 0.3$ (e.g. Salaris & Cassisi 1996) leading to a total metallicity $Z \approx 0.001$. The distance modulus (μ_V) reported in the table is an apparent (reddened) distance modulus; as is well known, it differs from the de-reddened one by $\approx 3.1\ E(B-V)$. As for the reddening, $E(B-V)$, inspection of Table 1 suggests that the reddening of M3 RR Lyrae is estimated to be very small.

We have considered the accurate database of 170 RR Lyrae light curves in the V and B bands provided by CC01. After exclusion of variables with Blazkho effect, with blended images or with an insufficiently precise determination of the period, one remains with 69 RR_{ab} and 19 RR_c covering the ranges of $\langle V \rangle$ magnitudes $15.476 \div 15.745$ and $15.291 \div 15.753$, respectively. To deal with a regular sequence of pulsators covering the whole color extension of the instability strip, we first selected from this sample the stars having $\langle V \rangle$ in the interval 15.60–15.70. We then chose variables with significantly different periodicities and light curve morphology. We ended with a sample of six stars (3 RR_c plus 3 RR_{ab}) which cover the range of $\langle B \rangle$–$\langle V \rangle$ spanned by the whole variable set. Then, in order to test the method on a significantly brighter object we added to the sample, the RR_c variable V152.

Table 2. Observed characteristics of the selected sample of variables. From left to right one finds the star identification, the period in days, the intensity averaged V magnitude, the intensity averaged $B-V$ color and the RR type.

Star	Period	$\langle V \rangle$	$\langle B \rangle - \langle V \rangle$	Type
V128	0.292	15.620	0.216	c
V75	0.314	15.626	0.240	c
V126	0.348	15.609	0.265	c
V72	0.456	15.679	0.247	ab
V6	0.514	15.686	0.285	ab
V120	0.640	15.676	0.384	ab
V152	0.326	15.496	0.201	c

Table 2 gives selected quantities for the final sample, whereas Fig. 1 shows the seven light curves. We notice that these variables cover a wide period range and are characterized by a variety of light curve morphologies. The possibility to model all these characteristics for consistent values of the intrinsic stellar parameters and distance represents a relevant test for the soundness of the theoretical pulsational scenario. Moreover the requirement that the distance values obtained for different pulsators are in agreement with each other within the uncertainties, further constrains the cluster distance.

2. Theoretical versus observed light curves

Model computations were performed by adopting $Z = 0.001$ $Y = 0.24$ and the same numerical and physical recipes that in BCM00 were found to provide an accurate modeling of field RR Lyrae and Classical Cepheid light curves (BCM02; Di Fabrizio et al. 2002; MC05). To transform theoretical light curves in the observational plane we adopted the atmospheric models by Castelli et al. (1997a,b). In Sect. 3 we show that plausible variations of the stellar metallicity and helium abundance does not affect in a relevant way the conclusions of the paper. However, when the evolutionary constraints are taken into account, our approach seems to exclude metal abundances as low as $Z = 0.0004$.

For RR_c pulsators, unless otherwise advised, the computations have been performed adopting for the mixing length parameter, governing the efficiency of the super-adiabatic convection and closing the system of nonlinear hydrodynamical equations in the pulsation code, the value $\alpha = 1.5$. This value has already been found to correctly reproduce the relevant pulsational properties of first overtone RR_c pulsators (e.g. M03; Di Criscienzo et al. 2004).

However previous investigations suggest that the α parameter should be increased when moving toward the red part of the instability strip reaching values as large as about 2.0 (BCM02; M03; Di Criscienzo et al. 2004; MC05). As we discuss later, this paper confirms that a mixing length value of $\alpha \approx 2.0$ is more suitable for the reproduction of RR_{ab} light curves, even when the effective temperature is as high as 7000 K. This does not occur for first overtone pulsators due to the more efficient damping of convection in the smaller mass involved in the pulsation mechanism (outside the first overtone radial node).

To reproduce an observed light curve with a given period, we assume the mass of the pulsator as almost a free parameter. As we discuss in Sect. 2.5, evolutionary calculations predict a quite restricted range for horizontal branch masses within the

instability strip. However, to be very conservative, as a first step, we allow a much wider mass range, namely $0.60 < M/M_\odot < 0.75$. For each given value of the mass, we explore the predicted light curves for selected luminosity levels. Once the mass and the luminosity are fixed, the effective temperature is determined by the constraint:
P(theoretical) = P(observed).

Adopting solar units for the stellar mass M and the luminosity L, the fundamental mode periods can be derived with good precision from the relation (MCDC03):

$$\log P = 11.066 + 0.832 \log L - 0.650 \log M - 3.363 \log T_e \quad (1)$$

which gives the connection between the variations in luminosity and in effective temperature, at fixed period and mass, for fundamental pulsators:

$$\Delta \log T_e = 0.247 \Delta \log L. \quad (2)$$

A similar relation is obtained for first overtone pulsators (MCDC03):

$$\log P = 10.673 + 0.805 \log L - 0.603 \log M - 3.281 \log T_e \quad (3)$$

which gives:

$$\Delta \log T_e = 0.245 \Delta \log L. \quad (4)$$

2.1. Variable V128

Figure 2 shows some results of the comparison among theoretical and observed light curves as applied to the variable V128, the first overtone pulsator with the shortest period in our sample. The labeled value of the distance modulus, *DM*, gives the vertical shift operated on the theoretical light curve to match the data, as reported in the various panels of the figure. From the left panels of Fig. 2 one sees that some theoretical light curves seem to reproduce quite satisfactorily the observed one, showing also the same characteristic flattening at the maximum luminosity. Thus it is worth defining a procedure to quantitatively evaluate the goodness of the match.

To do this we first evaluate the residuals as the difference between the observational and the theoretical light curves; these residuals are then fitted with a 10th order polynomial. The result is shown in the right panels of Fig. 2. We notice various cases in which the difference between theory and observations remains within 0.05 mag at each phase point. On the basis of this occurrence, for this variable, we decided to define as acceptable models those which match the observed data within 0.05 mag, also reproducing the observed morphology of the light curve. Moreover, we require that the predicted intensity weighted colors ($\langle B \rangle - \langle V \rangle$) agree with those observed within the observational uncertainties (~0.04 mag), as estimated by taking into account the photometric uncertainty and the error on the reddening.

As a whole, in the case of V128 one finds that pulsational theories are in perfect agreement with observations. In order to explore the response of the light curve to the structural parameters, Fig. 2 shows the results when the mass, the luminosity or the effective temperature are kept fixed. In particular, data in the bottom panels show that the shape of the curve is essentially a matter of effective temperature, with the other two parameters (M and L) only slowly affecting the pulsational amplitude. Such an occurrence can be easily interpreted in terms of the relevant role of the surface gravity. On this basis, one can easily understand that the relevant variations reported in both the top and the middle panels are mainly the consequence of variations in the effective temperature. Note that the short period of the first overtone pulsator V128 indicates that it is located close to the first overtone instability strip blue boundary. In order to keep a constant period, when increasing the luminosity we also have to increase the effective temperature (Eq. (4)), with the consequence that the amplitude decreases and the morphology becomes smoother, as expected when moving toward the instability strip blue boundary (Bono et al. 1997a).

The left top panel in Fig. 2 reveals that, if the mass is fixed at $M = 0.67\ M_\odot$, the fitting of the light curve appears able to formally discriminate the luminosity level within less than $\Delta \log L = 0.01$, i.e., within a few hundredths of magnitude. The right top panel shows the corresponding behavior of the difference between the observed and the theoretical curve, revealing that only for $\log L = 1.65$ $T_e = 7125$ K the discrepancy remains lower than ±0.05 mag at all pulsation phases.

The bottom panels show that keeping T_e constant, one finds an agreement within ±0.05 mag for masses in the range $M \approx 0.67$–$0.70\ M_\odot$.

To check if masses lower than $\approx 0.65\ M_\odot$ or higher than $\approx 0.71\ M_\odot$ provide worse fits for any possible combination of the stellar parameters, for each mass value outside these limits we explored the possible luminosity and effective temperature ranges, with the unique constraint to reproduce the observed period. The procedure is stopped at the smallest/largest mass for which no acceptable solution is found. The results are shown in Fig. 3, where, for fixed mass, the temperature range for stars inside the instability strip is uniformly spanned and the luminosity is changed according to Eq. (2).

We found that for masses larger than or equal to $M \approx 0.73\ M_\odot$, either the difference between theory and observation is higher than 0.05 mag. or, even when the observed pulsation amplitude is matched and the discrepancy remains within ±0.05 mag at any pulsation phase, the model is not able to accurately reproduce the morphology of the curve. On the other hand, for $M = 0.60\ M_\odot$, the assumed lowest limit in mass, we still obtain acceptable models for $\log L/L_\odot = 1.595$ and $\log L/L_\odot = 1.605$, respectively. Luminosities lower than $\log L/L_\odot = 1.595$ are not considered because they would imply a stellar mass lower than $0.60\ M_\odot$. We can also exclude luminosities higher than $\log L/L_\odot = 1.67$ because we have checked that at higher luminosity level models either do not fit the observed light-curve or do not present a stable pulsation limit cycle.

Figure 4 shows in the B band the comparison between observed data and the models reported in the bottom panel of Fig. 2. The quality of the fit in the B band is worse than in the V band with a maximum discrepancy of about 0.08 mag for the best fit cases. The apparent B distance moduli obtained are quite the same of the corresponding V ones and this result is consistent with the occurrence of a very low reddening. Figure 5 shows that, as in the V band comparisons, $M = 0.60_\odot$ is still an acceptable mass, while masses higher than $\approx 0.71\ M_\odot$ do not reproduce the observations.

However one should not forget that the pulsation amplitude also depends on the assumed value for the mixing length parameter $l/H_P = \alpha$. All these results have been obtained by adopting the standard mixing length parameter $\alpha = 1.5$, which, as noted above, is expected to correctly reproduce the relevant pulsational properties of RR_c. However, it is worth investigating the effect on the comparison between theoretical and observed light curves of small variations of the α parameter. As shown in Fig. 6, when the α value is increased at fixed mass, luminosity and effective temperature, the amplitude decreases (while a decrease of the α value has an opposite effect on the pulsational

amplitude). This trend is due to the quenching effect on pulsation, of the increased efficiency of convection (e.g. Stellingwerf 1982; BS94). However, the same amplitude might in principle be obtained with different α values if the stellar parameters are properly varied. On this basis we searched for additional solutions for $\alpha = 1.4$. Remembering that the main parameter affecting the light curve shape is the effective temperature of the star, different models with $\alpha = 1.4$ have been calculated (by requiring that the theoretical period exactly reproduces the observed ones) with a suitable fixed effective temperature, while the mass, and correspondingly, the luminosity, are varied according to Eq. (1) (see Fig. 7). We note that the ranges of acceptable stellar parameters and distance modulus, in the case of $\alpha = 1.4$, are almost the same as for the models with $\alpha = 1.5$. Figure 8 shows, analogously to Fig. 3, that at least one additional solution can be found for $M = 0.60\ M_{\odot}$, whereas no acceptable solutions are found for $M = 0.73\ M_{\odot}$. Moreover, as in the $\alpha = 1.5$ case, the theoretical reproduction of the observed data is slightly worse in the B band.

For α outside the range $1.4 \div 1.5$ we did not find any acceptable solutions. In particular, for $\alpha = 1.6$ it is possible to reproduce the light curve amplitude but not its morphology.

The first line of Table 3 shows the accepted ranges of mass, luminosity, effective temperature, intensity weighted $B-V$ color and apparent distance modulus. Other solutions with parameters within the ranges of Table 3 may exist but we verified that no solutions can be found outside these ranges. Data in Table 3 clearly show that while, as already discussed, the pulsational method is very sensitive to variations of the effective temperature, it is much less sensitive to mass changes; as we discuss in Sect. 2.5, indications to restrict the obtained mass range can come from evolutionary calculations. The distance moduli obtained are well within the range of the most recent estimates (see Table 1) and the theoretical colors are in agreement, within the uncertainties, with the empirical colors. The obtained distance modulus has an uncertainty of about ±0.1 mag. By taking into account the photometric error on the apparent magnitudes (~0.02 mag), our final estimate for the apparent distance modulus of V128 is $\mu_V{}^{V128} = 15.0 \pm 0.1$ mag.

2.2. Variable V126

Variable V126 is characterized by a longer period and a redder color than V128, but the apparent visual magnitude is identical within the photometric error. Following the same procedure as for V128, in the three panels of Fig. 9 we show the light curve shape of models calculated by fixing the mass, the luminosity and the effective temperature separately and varying the other two parameters, according to Eq. (3), to reproduce the observed period. We adopted $\alpha = 1.5$, as in the case for V128. All the trends found for V128 also hold for V126. In particular it is confirmed that the effective temperature is the key parameter to characterize the light curve morphology. Even in this case there are some models which reproduce the observed light curve within 0.05 mag. Therefore, as for V128, we decided to accept models for which the difference with the observation is within this limit and which reproduce the observed morphology. Following these criteria, the bottom panels of Fig. 9 seem to indicate $M \approx 0.63\ M_{\odot}$ as the highest acceptable mass. In fact, to check that there are not possible solutions for higher masses, we need to span, at fixed mass and with the requirement to reproduce the observed period, the whole range of possible effective temperatures (and thus luminosities). To check this point we calculated models for higher masses and several temperatures spanning the whole instability strip range, while the luminosity is fixed by Eq. (3). As shown in Fig. 10, it is possible to find acceptable solutions up to the highest mass we tested in our conservative approach ($M = 0.75\ M_{\odot}$). This is mainly due to the significantly larger intrinsic scatter of the light curve data with respect to the other selected pulsators, and also to the almost sinusoidal shape, which in principle can be easily reproduced by models close to the first overtone blue boundary.

Even if the $\langle B\rangle - \langle V\rangle$ color of the highest mass models are significatively lower than the observed values (see Table 3), taking into account the uncertainties in the color estimates, we conservatively decided to include these models.

The accepted ranges of mass, luminosity, effective temperature, apparent visual distance modulus and color are reported in the second line of Table 3. The large range of accepted mass values leads to a relatively wide range of luminosities and thus of distance modulus: $\mu_V^{V126} \approx 15.2 \pm 0.1$. The models in the bottom panels of Fig. 9 are shown in Fig. 11 in the B band. As for V128, the quality of the comparison between theory and observations is slightly worse than in the V band, but the obtained results are consistent. The colors of the accepted models for V126 (but the already discussed highest mass models) are in agreement with the observed values and the difference between the inferred apparent B and V distance moduli is consistent with a very low reddening value.

In the previous section we have shown for V128 that small variations of the α parameter (higher variations are not allowed as a result of the requirement to reproduce the observed light curve morphology and period) do not significantly change the accepted range of stellar parameters. We checked that this is true also for V126.

Regarding the stellar parameters, we find indications for an effective temperature possibly lower than that of V128, as expected on the basis of the observed colors and periods; whereas the predicted luminosity could be brighter than that estimated for V128. These results could suggest a small evolutionary effect for V126 as is also possibly indicated by the evidence that this RR_c pulsator is redder than 7 RR_{ab} variables in the same sample. However, the observed apparent visual magnitude is the same as that of V128 within the photometric error (see Table 2) so that, even taking into account the effect of bolometric corrections, the two pulsators should have similar intrinsic luminosities.

2.3. Variable V72

Variable V72 is a fundamental pulsator with an intensity weighted $B - V$ color intermediate between those of the RR_c V126 and V128, likely close to the blue boundary of the fundamental instability strip. This assumption is also supported by the large amplitude of its visual light curve. In order to find possible theoretical models for this fundamental variable we adopted the same method as for the RR_c pulsators. Indeed, as expected (see the discussion in Sect. 2), the best agreement is not obtained for $\alpha = 1.5$ (see Fig. 12). The best match is found when α is increased to 2.0, and by assuming a non-vanishing overshooting efficiency in the regions in which the superadiabatic gradient is negative (see Eq. (7) and Sect. 3 in BS94). Given the higher and more asymmetric shape of fundamental light curves, the agreement between the observed and theoretical light curve is not within the 0.05 mag level at all phase points, as in the V128, V126 cases. At most we find an agreement within ±0.08 mag. Therefore we consider as acceptable models for V72, those which show a difference with observations ≤0.08 mag at all the phase points.

Table 3. Accepted ranges of the physical parameters (mass, luminosity and effective temperature) for variables V128, V126, V72 and V152, together with the corresponding range of apparent visual distance modulus and intensity weighted $(B-V)$ color. For the V152 variable the range in temperature (color) has not been calculated (see text).

Variable	Mass $[M_\odot]$	$\log (L/L_\odot)$	T_e [K]	μ_V [mag]	$\langle B\rangle - \langle V\rangle$ [mag]
V128	0.60 ÷ 0.71	1.595 ÷ 1.670	7050 ÷ 7150	14.92 ÷ 15.11	0.227 ÷ 0.240
V126	0.60 ÷ 0.75	1.683 ÷ 1.775	7020 ÷ 7080	15.12 ÷ 15.35	0.235 ÷ 0.244
V72	0.60 ÷ 0.73	1.643 ÷ 1.710	6900 ÷ 7000	15.04 ÷ 15.22	0.227 ÷ 0.237
V152	0.60 ÷ 0.69	1.666 ÷ 1.711		14.94 ÷ 15.04	

The variations of the light curve characteristics at fixed mass, luminosity and effective temperature are shown in the three panels of Fig. 13. The dependence on the physical parameters is similar to that already discussed for V128 and V126.

We note that for V72 we were not able to find equivalently good solutions for α lower or higher than 2.0. The accepted ranges of the physical parameters, apparent distance modulus and color are reported in the third line of Table 3. In particular we find $\mu_V \approx 15.1 \pm 0.1$. Also in this case we checked that there are no acceptable models outside these ranges. In order to check that $M = 0.74\ M_\odot$ really represents the upper limit of the acceptable mass values, we computed models (see Fig. 14) for this mass, varying the luminosity and the effective temperature with the constraint of reproducing the observed period. The plot shows that for $M = 0.74\ M_\odot$ there are no possible solutions. We also verified that no solution is found for a luminosity higher than $\log L/L_\odot \approx 1.71$ (see Fig. 15). These tests allow us to confirm the obtained range for the distance modulus. The fact that searching either for mass limits or for luminosity limits one obtains the same range of physical parameters is a consequence of Eqs. (1) and (3).

Figure 16 shows the models of the bottom panel of Fig. 13 in the B band. As for the RR_c pulsators, the agreement between theory and observations in the B band is slightly less accurate with respect to that in the V band, suggesting that we should assume as acceptable a discrepancy theory-observation within 0.1 mag. Similar results are obtained for the equivalent situation in the B band of Figs. 14 and 15.

On the basis of the results obtained so far for V128, V126 and V72, we estimate a mean apparent distance modulus $\mu_V = 15.1 \pm 0.1$ mag.

At the end of this section we discuss problems which arose in the analysis of the RR_{ab} variable V120, a fundamental pulsator with a quite red color and a relatively long period, likely close to the red boundary of the fundamental instability strip. For the very red RR Lyrae, the modeling of the light curve morphology already appears problematic (see e.g. MC05). This is probably due to the remaining uncertainties in the treatment of the coupling between pulsation and convection in the hydrodynamical models. In particular theoretical light curves for red pulsators can show a spurious feature before the maximum (see e.g. the atlas reported in Bono et al. 1997a,b) which is not observed in real curves, even if the pulsation amplitude is well reproduced.

For V120 we are not able to find acceptable solutions even allowing the physical parameters and the α values to vary over wide ranges. Figure 17 shows, as an example, some attempts to find possible solutions. A detailed investigation of this problem and of its dependence on variations of the parameters entering in the turbulent convective models will be addressed in a forthcoming paper.

2.4. The variables V75, V6

The light curves of the two pulsators, namely the RR_{ab} V6 and the RR_c V75, show morphological features similar to those of the pulsators discussed above. For this reason we do not present the same detailed analysis of the dependence of results on the model input parameters, but we show one of the possible solutions for each object. The α value adopted to obtain a good reproduction of the observed light curve is, in agreement with the previous pulsation models, $\alpha = 1.5$ for the RR_c and $\alpha = 2.0$ for the RR_{ab}. These results are shown in Fig. 18. We note that the predicted values for the physical parameters and the distance modulus are within the range shown in Table 3. Similar results are obtained for the B band.

2.5. Comparison with evolutionary model results

The pulsational results can be compared with evolutionary model predictions. To this end, we adopted the Zero Age Horizontal Branch (ZAHB) properties for $Z = 0.001$, as reported in recent papers, as based on different assumptions concerning the original helium abundance, the set of physical inputs (radiative and conductive opacities, EOS tables, nuclear reactions rates, neutrino energy losses etc.) and the efficiency of the external convection. The adoption of different evolutionary predictions allows us to obtain a rough estimate of the uncertainty on current stellar models. By comparing the obtained ranges of pulsational mass and luminosities, corresponding to a given effective temperature, with the same results for the evolutionary models, one can roughly evaluate the consistency between the two theories. As already discussed, pulsation models are very sensitive to the effective temperature, with the consequence that the estimated effective temperature range is quite small. Due to the significantly lower sensitivity of evolutionary predictions on this parameter and to the unavoidable uncertainty in the evolutionary predictions for this quantity, a mean value for the theoretical effective temperature of all the variables taken into account in our analysis, namely $T_e \approx 7000$ K, can be used. Table 4 summarizes the evolutionary values for masses and luminosities by the different quoted authors, corresponding to the selected temperature value. All results are within the pulsational ranges given in Table 3. It is also worth noting that the pulsational calculations are less sensitive than the evolutionary ones to masses and luminosities. However, the evidence that two completely independent methods give consistent results is encouraging, in spite of the several possible uncertainty sources in both the evolutionary and pulsational calculations. Finally, we note that for some variables off-ZAHB evolution effects can be not negligible, producing luminosities higher by about 0.1 dex, for a fixed effective temperature. By taking into account the evolutionary predictions reported in Table 4 and the possibility of off-ZAHB evolution, we can restrict the ranges reported in Table 3, discarding all masses lower than $\sim 0.62\ M_\odot$ and higher than $\sim 0.67\ M_\odot$. This

Table 4. Evolutionary masses and luminosities predicted by different sets of ZAHB models for a mean effective temperature of 7000 K, obtained from our best fit pulsational models (see text). The selected evolutionary papers are: V00, VandenBerg et al. (2000); DC02/C05, D'Antona et al. (2002) and V. Caloi (2005, private communication quoted in MC05); P04, Pietrinferni et al. (2004); CDC04, Cariulo et al. (2004).

Author	Mass $[M_\odot]$	log $L/L_\odot$
V00	0.63	1.65
DC02/C05	0.645	1.67
P04	0.64	1.67
CDC04	0.65	1.68

selection implies that the ranges of the inferred individual distance moduli are significant reduced, giving a weighted mean value of 15.08 ± 0.02 mag.

2.6. Results for a brighter pulsator

Until now, as discussed in the introduction, we have analyzed variables in a restricted range of luminosity, to deal with a sequence of pulsators spanning the temperature range of the predicted instability strip, at a given luminosity level. As already discussed, for each variable, we found a range of physical values (and thus distance moduli) which are in agreement within each other.

A further check of the reliability of the estimated cluster distance modulus is to analyze the properties of pulsators with a different luminosity: as these stars are also cluster members, the obtained distance modulus has to be in agreement with the previous results.

To this aim we selected the RR_c V152, which has a well-sampled light curve in the V and B bands and is brighter by $\approx$0.1 to 0.2 mag than the other selected variables (see Table 2). It takes into account firstly the above-mentioned evidence that the temperature is the key parameter for good agreement between the theory and observations, and secondly that the expected mass, luminosity and distance modulus ranges are essentially obtained by investigating the quality of the comparison between the theory and observations at a fixed effective temperature. Figure 19 shows the results for models of different mass (luminosity) with a suitable temperature value (T_e = 7087 K). We selected as acceptable models those for which the difference with the observations is within 0.05 mag at all the pulsation phases. We also checked that even if the temperature is allowed to vary, $M = 0.71\ M_\odot$ really represents the upper limit in mass (see Fig. 20). Similar to what was obtained for the other variables, the conclusions are the same when the comparison is performed in the B band.

The ranges obtained of mass, luminosity and distance modulus are shown in Table 3. We note that the distance modulus range for this brighter pulsator is consistent with results obtained for the other variables, even if the visual magnitude is higher. A similar agreement is obtained for the stellar mass and luminosity.

Including V152 in our sample and taking into account the evolutionary constraints discussed in the previous section, we obtain a weighted mean distance modulus of 15.05 ± 0.02 mag.

3. Chemical composition effects

As mentioned above, all calculations have been performed for a metallicity value $Z = 0.001$ and a helium abundance $Y = 0.24$. We discuss here how our results are affected by the assumed chemical composition. In previous papers (e.g. Bono et al. 1996, BCM00) we have shown that the shape of light curves is affected by metallicity, with a minor dependence on the Helium content (see Bono et al. 1997a). To check how this dependence can affect our estimates of the stellar intrinsic parameters and distance, we calculated some additional models for a significantly lower metallicity value, which is outside the range of metallicity values indicated in the literature for M3, namely $Z = 0.0004$. Figure 21 shows that, at least for variable V128, in spite of a change in the best fit model intrinsic parameters, we are able to find solutions with mass, luminosity (and thus distance modulus) within the previous accepted ranges of Table 3. A slight increase of the effective temperature is needed, confirming that the temperature is a key parameter affecting the morphology and the amplitude of RR Lyrae light curves. However, in the comparison with the evolutionary prescriptions (see Sect. 2.5) we have to consider that for $Z = 0.0004$ the expected stellar masses on the ZAHB (around T_e = 7000 K) are about 0.7 $M_\odot$. This implies that the models fitting the observations within $\pm$0.05 in Fig. 21 should be excluded. From this perspective, our approach seems to confirm the most recent spectroscopic measurements, which exclude for M3 a metallicity as low as $Z = 0.0004$.

Regarding the helium abundance, within reasonable variations of the relative helium to metal enrichment ratio ($1.0 \leq \Delta Y/\Delta Z \leq 6.0$) and assuming a primordial helium content no larger than 0.24, we do not find any significant effect on the predicted light curves.

4. The observed light curves by Hartman et al. (2005) and Benkő et al. (2006)

Recently Hartmann et al. (2005) published three bands (BVI) light curves for several variables of different types in M3; in particular all the variables selected by us, except V126, are included in the Hartmann et al. (2005) sample. Moreover during the completion of this study another paper on the light curves of the M3 RR Lyrae in the V, B and I photometric bands was published (Benkő et al. 2006) in which all the light curves selected in our paper are analyzed. Figure 22 shows the comparison of the V, B and I data by Hartmann et al. (2005) and Benkő et al. (2006) with those by CC01 for all our analyzed variables.

Regarding the V band we note that the light curves by the different authors are almost coincident or vertically shifted by only a few hundredths of magnitude, an amount which is within the errors due to photometric uncertainties and the fitting procedure. A similar agreement is found in the B and I bands. We also note that the periods quoted by Hartmann et al. (2005) and Benkő et al. (2006) for the selected variables are the same as those by CC01.

From Fig. 22 it is clear that the theoretical models which reproduce the CC01 B and V light curves are also able to match the Hartmann et al. and the Benkő et al. data with, at most, a slight variation of the distance modulus, still consistent with the results of Table 3 within the errors.

To investigate if the data in the I band confirm the results obtained in the V and B bands, Fig. 23 shows the comparison between the models corresponding to the bottom panels of Fig. 2 (for V128) and Fig. 13 (for V72) and the data by Hartmann et al. in the I band. We note that the agreement between theory and observation is good (within 0.05 mag), thus confirming the results obtained in the previous section. Moreover the apparent distance moduli obtained for the V and I bands are very similar, confirming the occurrence of a low reddening value. Similar results

Table 5. Physical parameters of V128, V126 and V72 variables as derived by Cacciari et al. (2005) from color-temperature calibration.

Star	Mass $[M_\odot]$	T_e [K]	$\log L/L_\odot$
V128	0.67 ± 0.05	7228 ± 100	1.681 ± 0.03
V126	0.70 ± 0.05	6855 ± 100	1.692 ± 0.03
V72	0.72 ± 0.05	6773 ± 100	1.670 ± 0.03

are obtained for the other selected variables for which I data are available.

5. Comparison with the results by Cacciari et al. (2005)

In a recent paper, Cacciari et al. (2005) performed a detailed study of the pulsational and evolutionary characteristics of 133 RR Lyrae stars in M3. On this basis physical parameters were derived from $B - V$ colors and accurate color-temperature calibrations, as well as from Fourier coefficients. The results obtained from the color-temperature calibration, which are considered by the authors themselves to be more precise than those based on the Fourier parameters, are reported in Table 5.

By comparing these values with the ranges reported in Table 3 we see that an agreement for the intrinsic stellar parameters can be found, within the error bars, for all the variables, even if in some cases the overlap between the ranges proposed by Cacciari et al. and those obtained in the present work is marginal.

6. Final remarks

We have successfully modeled the light curves of six variables (four RR_c and two RR_{ab}) of the globular cluster M3.

For four variables (V128, V126, V72, V152), spanning a significant period range and showing different light curve morphologies, we searched for multiple solutions analyzing the dependence of the theoretical light curves on the model input parameter. We remark that, due to the degeneracy inherent to the method, from the theoretical reproduction of the observed light curve of a given variable one can obtain only a range of stellar parameters; the analysis of several variables belonging to the same cluster allows us to provide sounder constraints and also mean results. To our knowledge, this is the first time that such an analysis has been done in a systematic way.

The obtained acceptable ranges of stellar parameters (mass, luminosity and effective temperature) and distance modulus are self-consistent and in agreement with stellar evolutionary predictions. Moreover a general agreement can be found with the physical parameters provided by Cacciari et al. (2005), on the basis of a multicolor study. For the other two pulsators (V75 and V6), that show morphological features similar to the previous ones, the obtained stellar parameters and distance moduli are consistent with the previously-identified ranges, confirming the previous estimates. These results represent a check for both evolutionary and pulsational theories.

The failure in the reproduction of the light curve morphology for the reddest pulsator V120, likely due to some remaining uncertainties in the adopted turbulent convective models, represents a challenge for future model developments.

Our final estimate for the distance modulus is $\mu_V = 15.1 \pm 0.1$, derived as a mean of the individual determinations, while taking also into account the evolutionary constraints on the pulsator masses, obtains a weighted mean value of 15.05 ± 0.02.

Our obtained distance modulus is consistent, within the uncertainties, with the results from other methods, for example with the determination by Ferraro et al. (1999), obtained from the comparison between the observed and predicted Zero Age Horizontal Branch luminosity, as well as with the results by M03, based on additional pulsational methods (see their Table 4). The precision of the technique could be further improved if accurate radial velocity curves are available together with photometric data covering both the optical and the near-infrared bands.

Acknowledgements. This paper is dedicated to the memory of V. Castellani who inspired this work and constantly supported us. We shall miss his personality, clearness and enthusiasm in approaching the different issues of stellar astrophysics. We are grateful to P. G. Prada Moroni and S. Shore for careful reading of the manuscript and to F. Caputo for useful suggestions. We are grateful to the anonymous referee for her/his suggestions and comments which greatly improved the paper. Financial support for this work was provided by MIUR under the scientific projects "Continuity and discontinuity in the Galaxy formation" (P.I.: R. Gratton) and "On the evolution of stellar systems: a fundamental step toward the scientific exploitation of VST" (P.I.: M. Capaccioli).

References

Benkő, J. M., Bakos, G. Á., & Nuspl, J. 2006, MNRAS, 372, 1657
Bono, G., & Stellingwerf, R. F. 1994, ApJS, 93, 233 (BS94)
Bono, G., Incerpi, R., & Marconi, M. 1996, ApJ, 467, l97
Bono, G., Caputo, F., Castellani, M., & Marconi, M. 1997a, A&AS, 121, 327
Bono, G., Caputo, F., Cassisi, S., Castellani, V., & Marconi, M. 1997b, ApJ, 479, 279
Bono, G., Castellani, & Marconi, M. 2000, ApJ, 532, L29 (BCM00)
Bono, G., Castellani, V., & Marconi, M. 2002, ApJ, 565, L83 (BCM02)
Buonanno, R., Corsi, C. E., Buzzoni, A., Cacciari, C., et al. 1994, A&A 290, 69
Cacciari, C., Corwin, T. M., & Carney, B. W. 2005, AJ, 129, 267
Carretta, E., & Gratton, R. 1997, A&AS, 121, 95
Cariulo, P., Degl'Innocenti, S., & Castellani, V. 2004, A&A, 421, 1121
Castellani, V., Degl'Innocenti, S., & Marconi, M. 2002, in Omega Centauri, A Unique Window into Astrophysics, ed. F. van Leeuwen, J. D. Hughes, & G. Piotto, ASP Conf. Proc., 265, 193
Castellani, V., Castellani, M., & Cassisi, S. 2005, A&A, 437, 1017
Castelli, F., Gratton, R., & Kurucz, R. L. 1997a, A&A, 318, 841
Castelli, F., Gratton, R., & Kurucz, R. L. 1997b, A&A, 324, 432
Catelan, M. 2004, ApJ, 600, 409
Clement, C. M., Muzzin, A., Dufton, Q., et al. 2001, AJ, 122, 2587
Clementini, G., Corwin, T. M., Carney, B. W., & Sumerel, A. N. 2004, AJ, 127, 938
Corwin, T. M., & Carney, B. W. 2001, AJ, 122, 3183 (CC01)
D'Antona, F., Caloi, V., Montalban, J., et al. 2002, A&A 395, 69
Di Criscienzo, M., Marconi, M., & Caputo, F. 2004, ApJ, 612, 1092
Di Fabrizio, L., Clementini, G., Marconi, M., et al. 2002, MNRAS, 336, 841
Ferraro, F. R., Messineo, M., Fusi Pecci, F., et al. 1999, AJ 118, 1738
Feuchtinger, M. U. 1999, A&AS, 136, 217
Gehmeyr, M. 1992, ApJ, 399, 272
Gehmeyr, M. 1993, ApJ, 412, 341
Harris, W. E. 2003, updated version of Harris W. E. 1996, AJ, 112, 1487 at the URL `http://physwww.physics.mcmaster.ca/`
Hartman, J. D., Kaluzny, J., Szentgyorgyi, A., & Stanek, K. Z 2005, AJ, 129, 1596
Jurcsik, J., Benko, J. M., Bakos, G. Á., et al. 2003, ApJ, 597, L49
Keller, S. C., & Wood, P. R. 2002, ApJ, 578, 144
Keller, S. C., & Wood, P. R. 2006, ApJ, 642, 834
Marconi, M., & Clementini, G. 2005, AJ, 129, 2257 (MC05)
Marconi, M., Caputo, F., Di Criscienzo, M., & Castellani, M. 2003, ApJ, 596, 299 (M03)
Pietrinferni, A., Cassisi, S., Salaris, M., & Castelli, F. 2004, ApJ, 612, 168
Rood, R. T., Carretta, E., Paltrinieri, B., et al. 1999, ApJ, 523, 752
Salaris, M., & Cassisi, S. 1996, A&A 305, 858
Stellingwerf, R. F. 1982, ApJ, 262, 339
Thompson, I. B., Kaluzny, J., Pych, G., et al. 2001, AJ, 121, 3089
VandenBerg, D. A., Swenson, F. J., & Rogers, F. J. 2000, ApJ, 532, 430
Wood, P. R., Arnold, A., & Sebo, K. M. 1997, ApJ, 485, 25 (WAS)
Zinn, R., & West, M. J. 1984, A&AS, 55, 45

Online Material

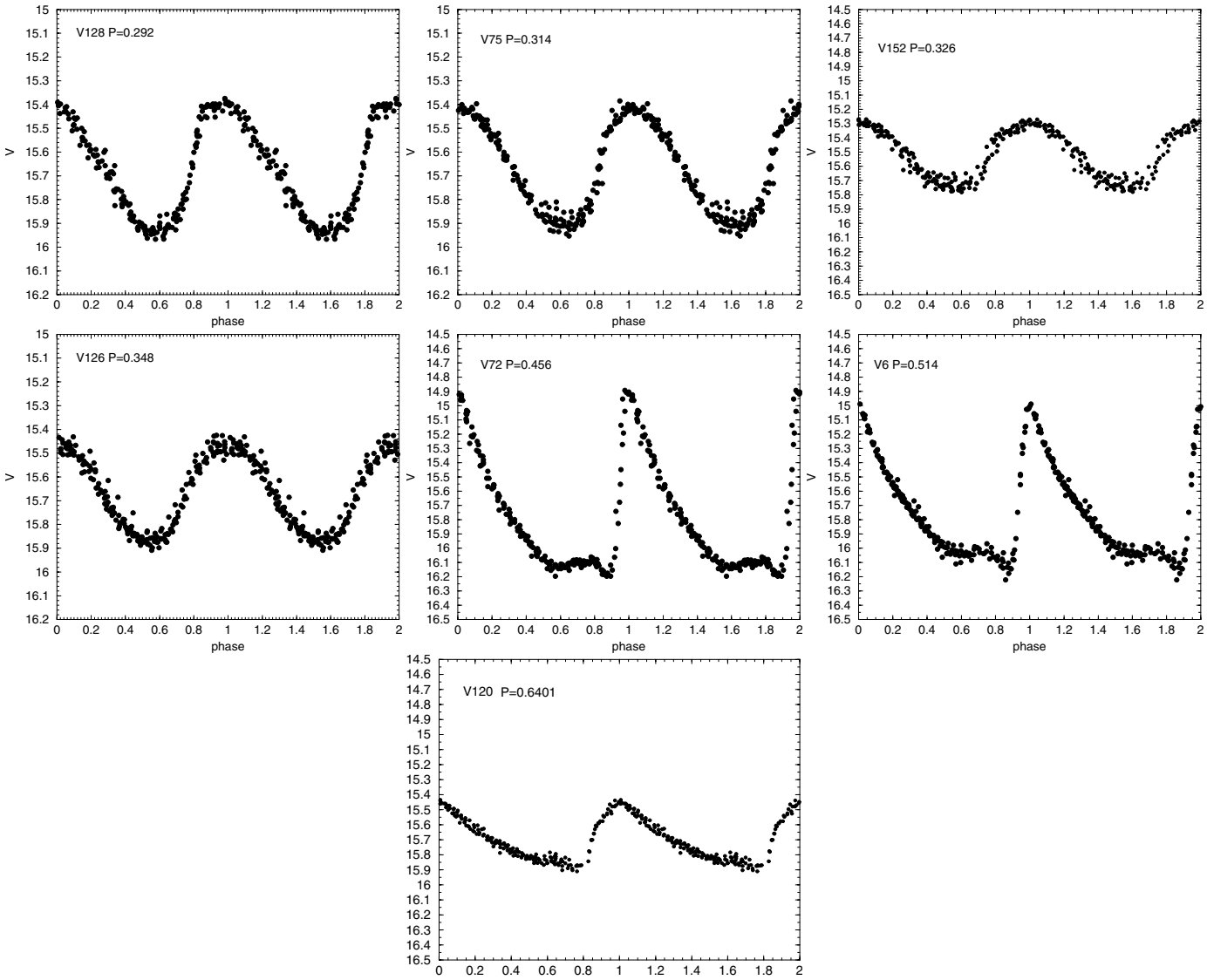

Fig. 1. Observational data in the *V* band for the selected light curves, from Corwin & Carney (2001). Periods (in days) are labeled.

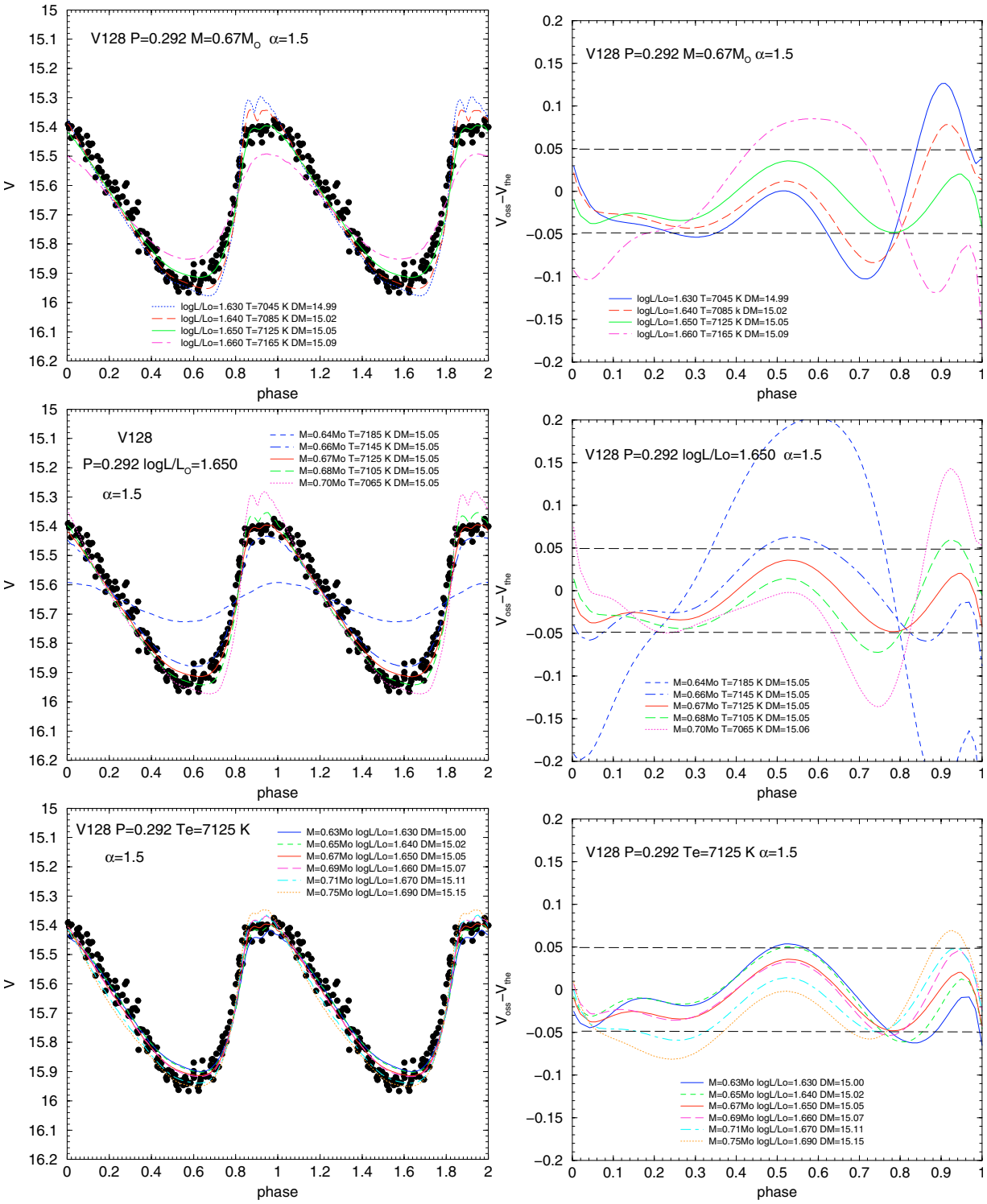

Fig. 2. Predicted light curves constrained to the observed period of V128 for the labeled fixed values of mass (*top panel*), luminosity (*middle panel*) and effective temperature (*bottom panel*). The *right panels* show the differences between theory and observations, computed as described in the text.

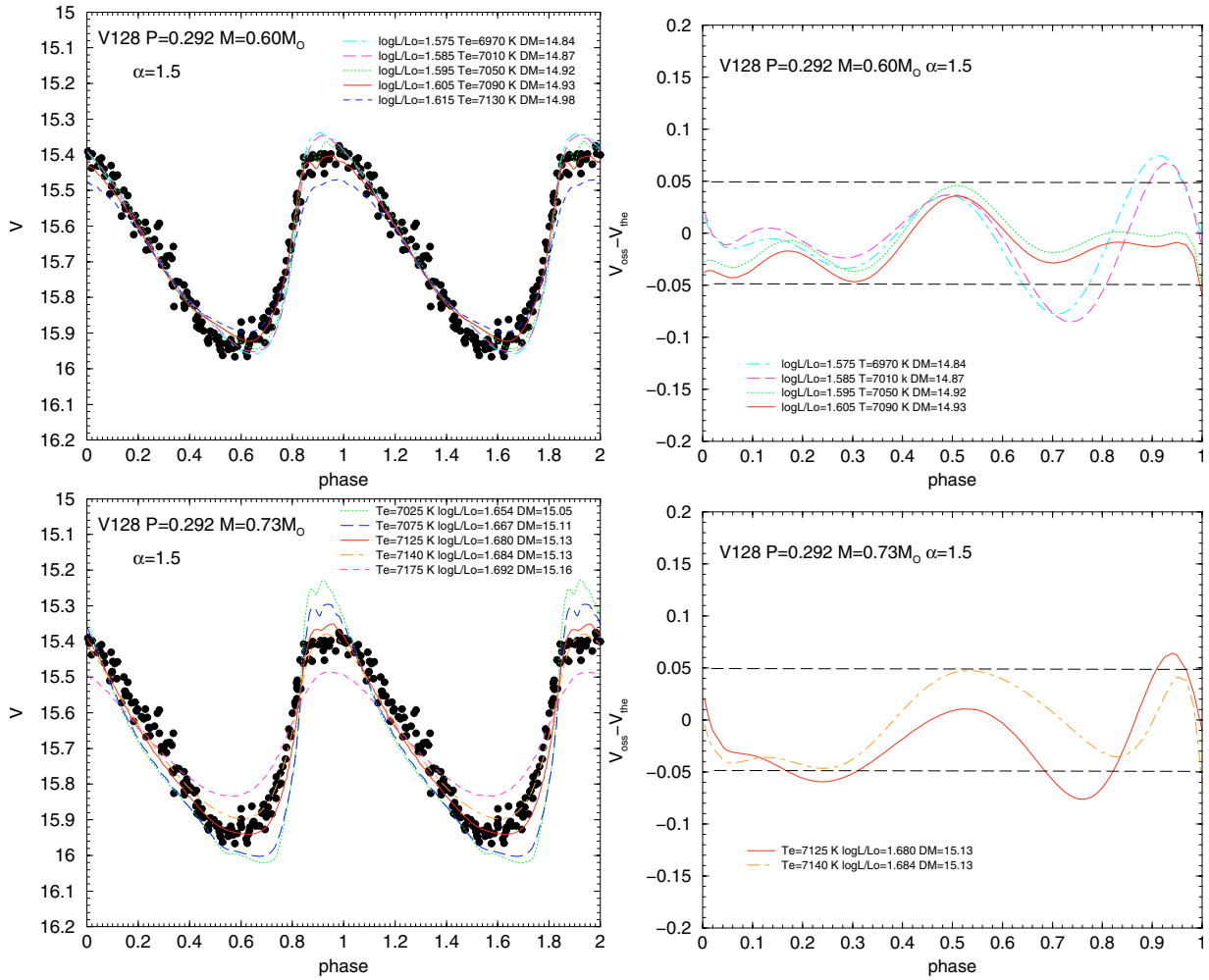

Fig. 3. Predicted light curves constrained to the observed period of V128 for two different mass values, namely $M = 0.60\ M_\odot$ (*left upper panel*) and $M = 0.73_\odot$ (*left lower panel*). The temperature range for stars inside the first overtone instability strip is uniformly spanned. The *right panels* show the fit residuals for the corresponding models.

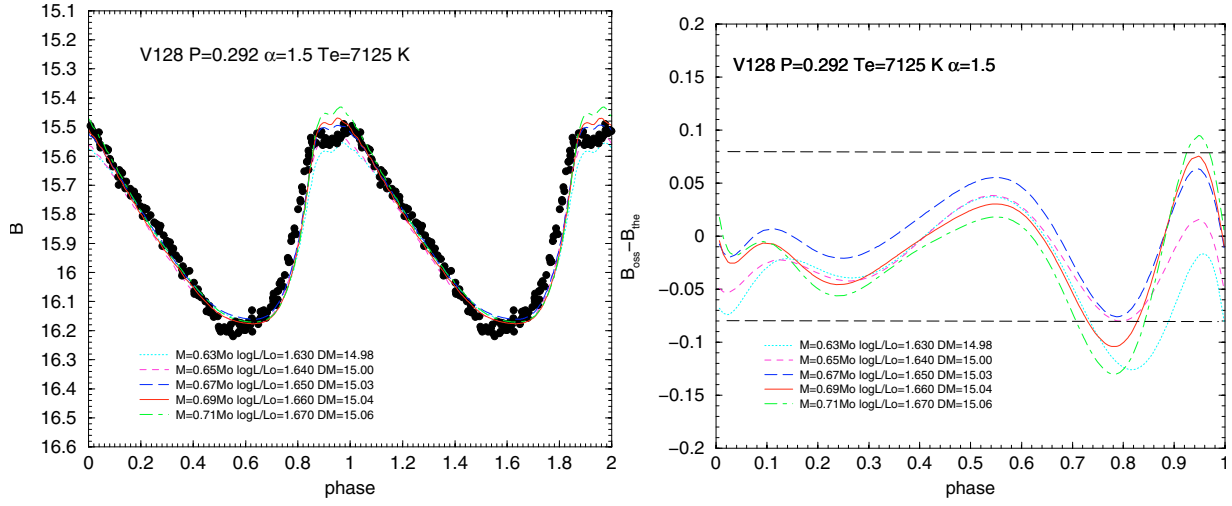

Fig. 4. As in the bottom panel of Fig. 2 but for the *B* band.

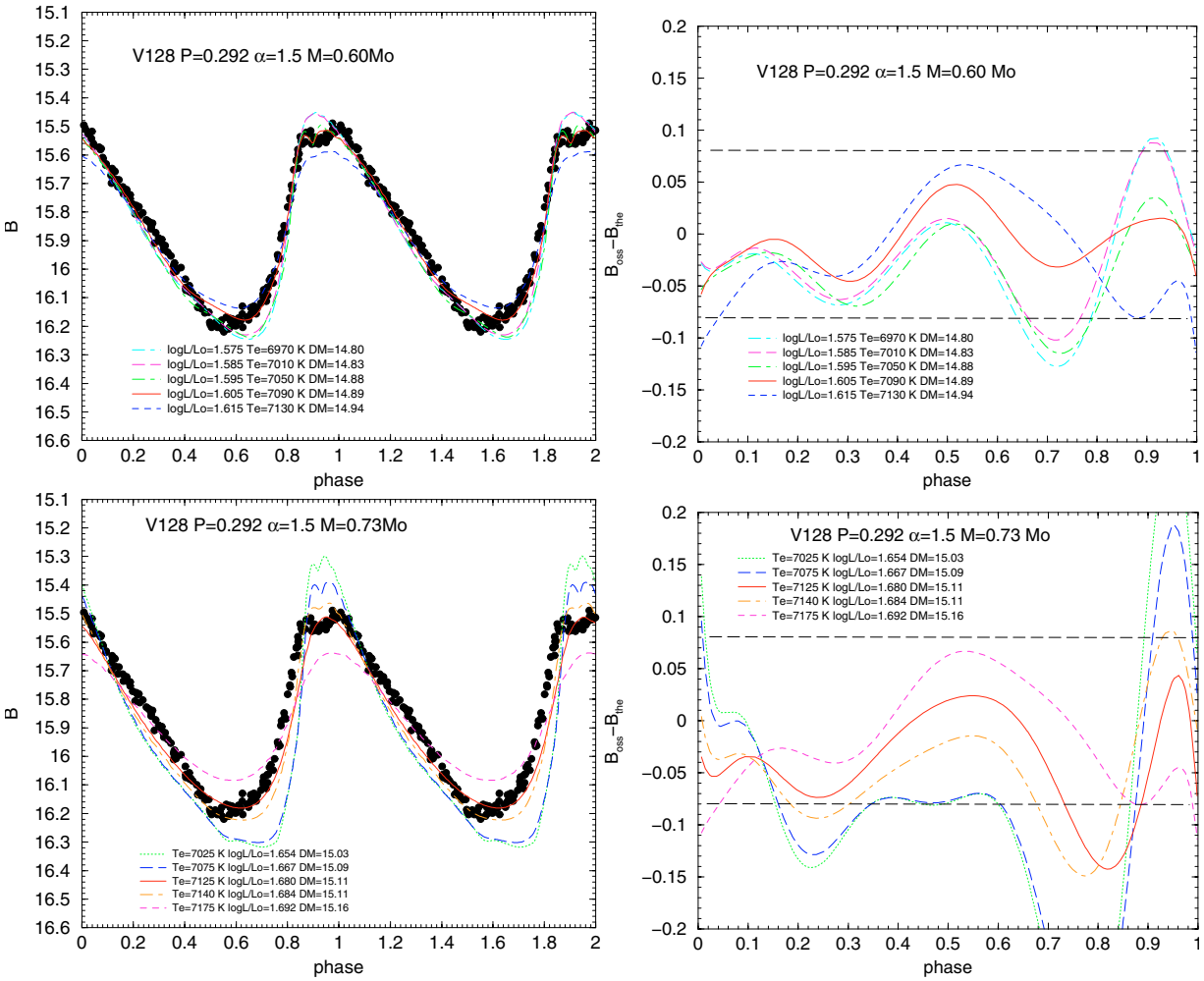

Fig. 5. The same as Fig. 3 but in the *B* band.

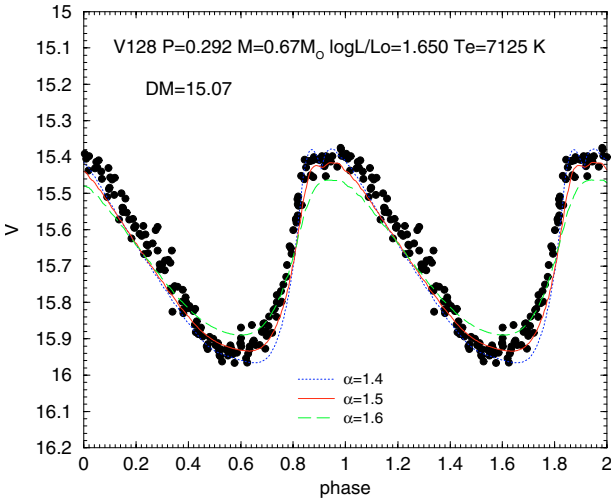

Fig. 6. The behavior of the light curve shape for the V128 fitting case, when the α parameter is slightly varied at fixed mass, luminosity and effective temperature.

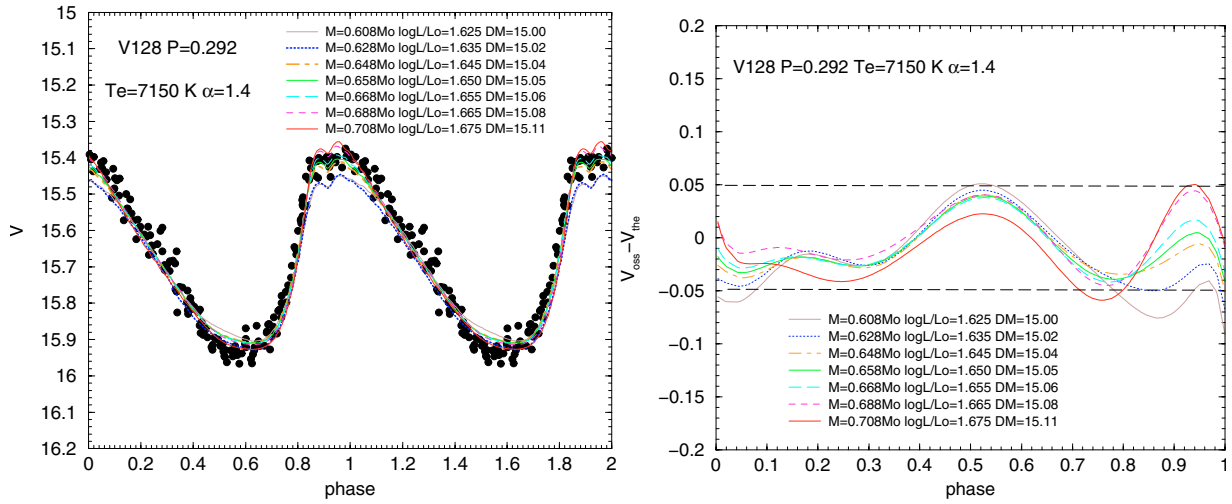

Fig. 7. As in the *bottom panel* of Fig. 2 but for $\alpha = 1.4$ and a suitable value of effective temperature (see text).

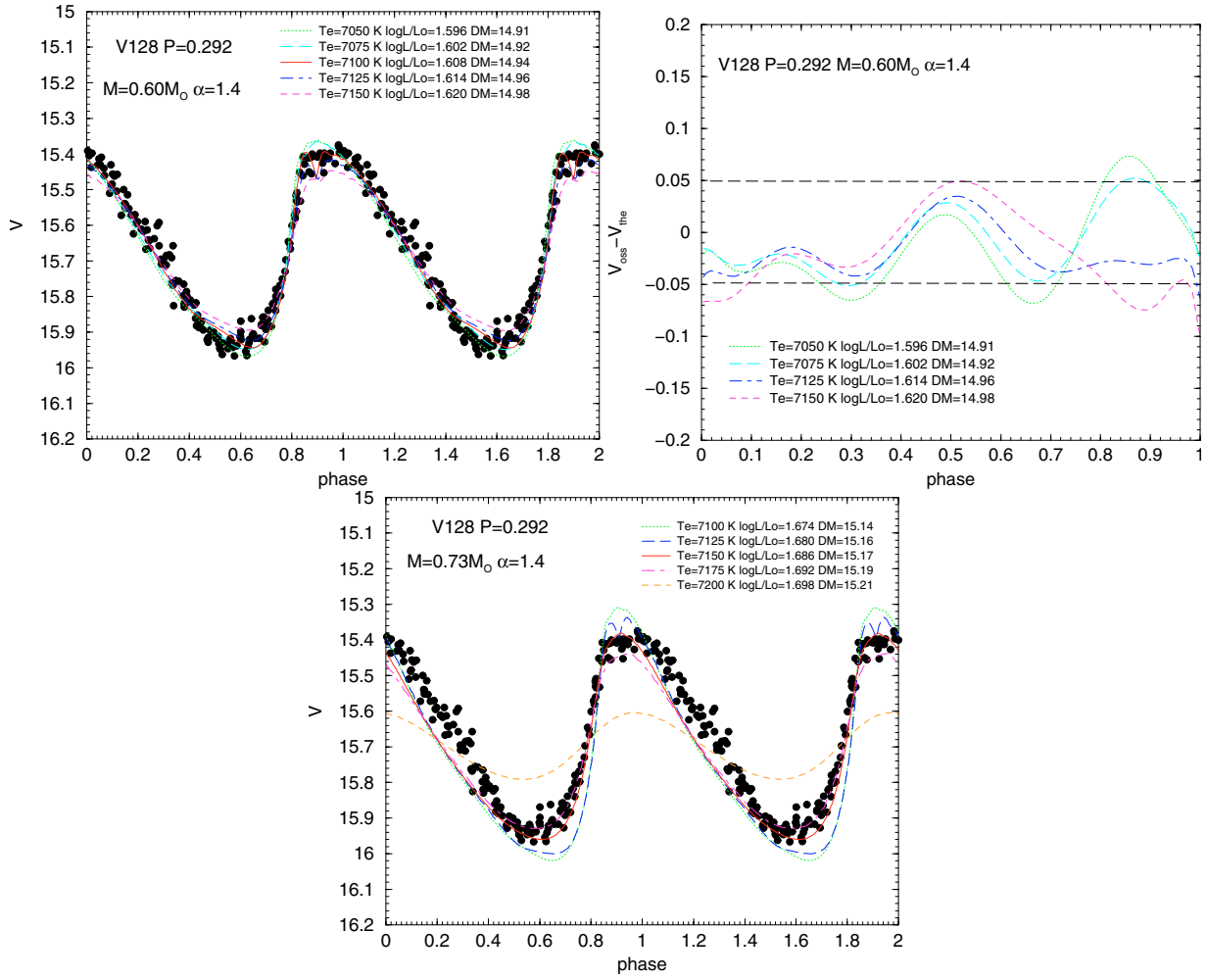

Fig. 8. As in Fig. 3 but for $\alpha = 1.4$.

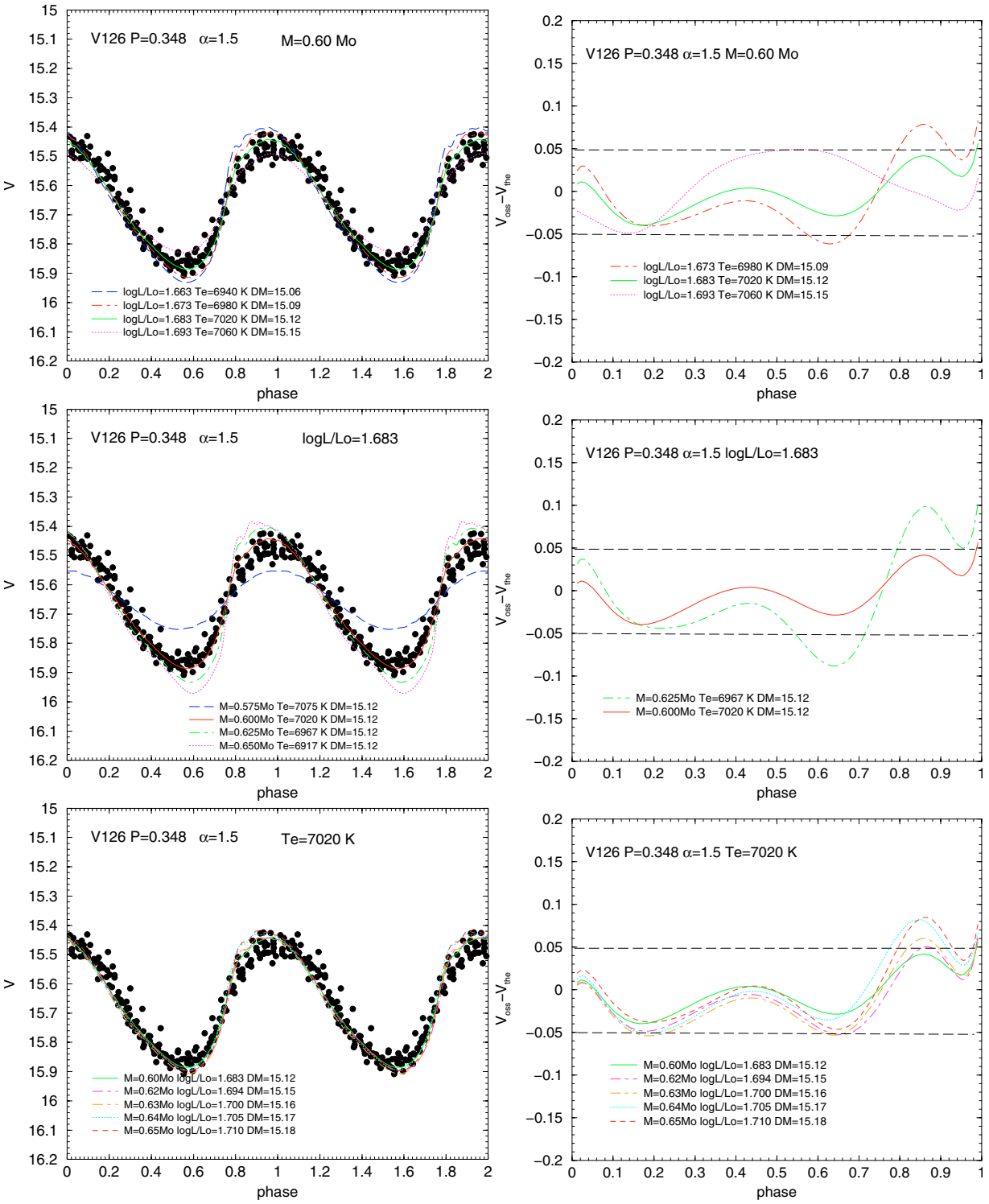

Fig. 9. As in Fig. 2 but for the variable V126.

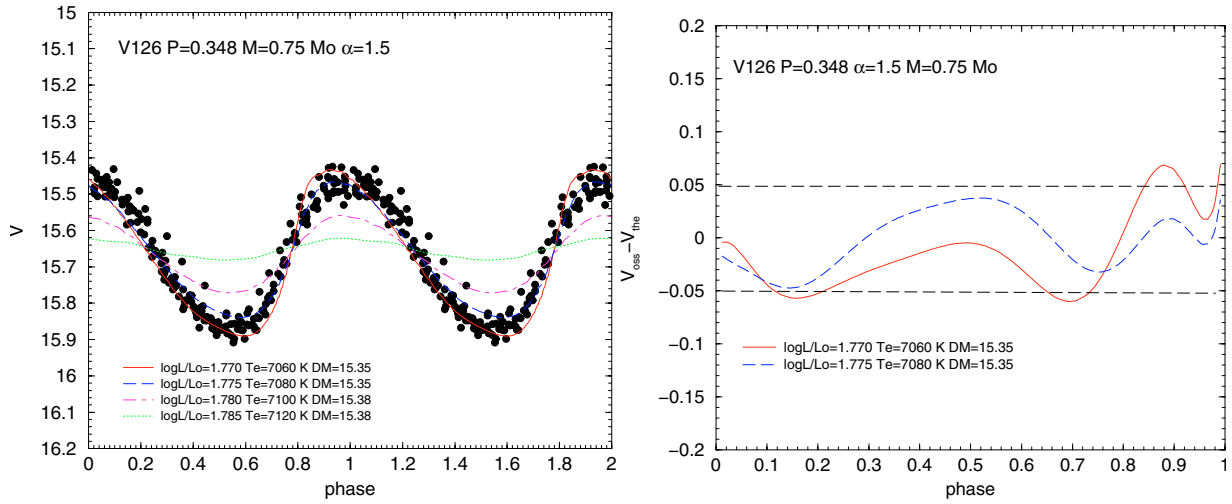

Fig. 10. Predicted light curves constrained to the observed period of V126 for $M = 0.75 M_{\odot}$. The temperature range for stars inside the first overtone instability strip is uniformly spanned.

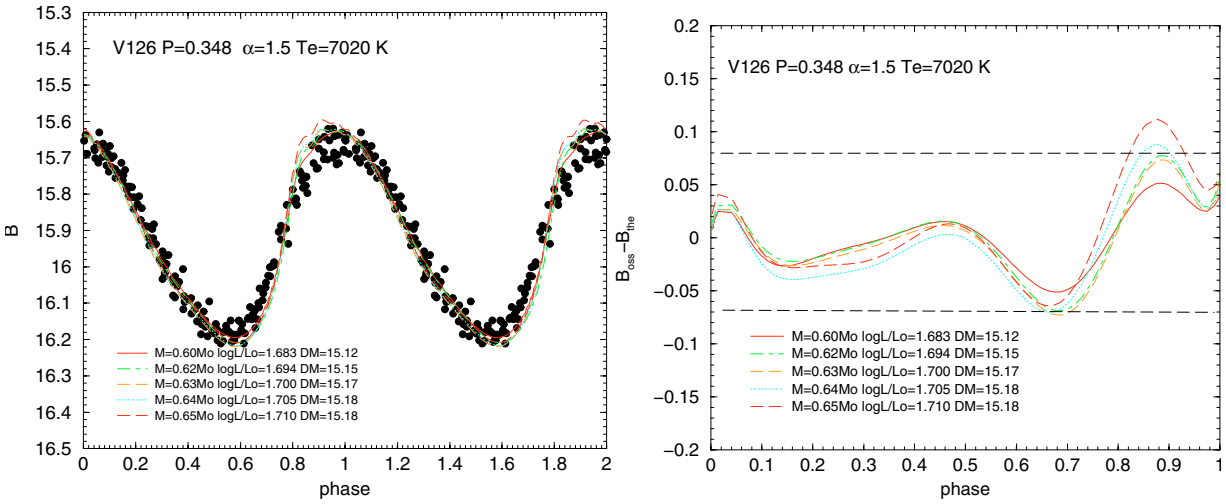

Fig. 11. As in the *bottom panel* of Fig. 9 but for the *B* band.

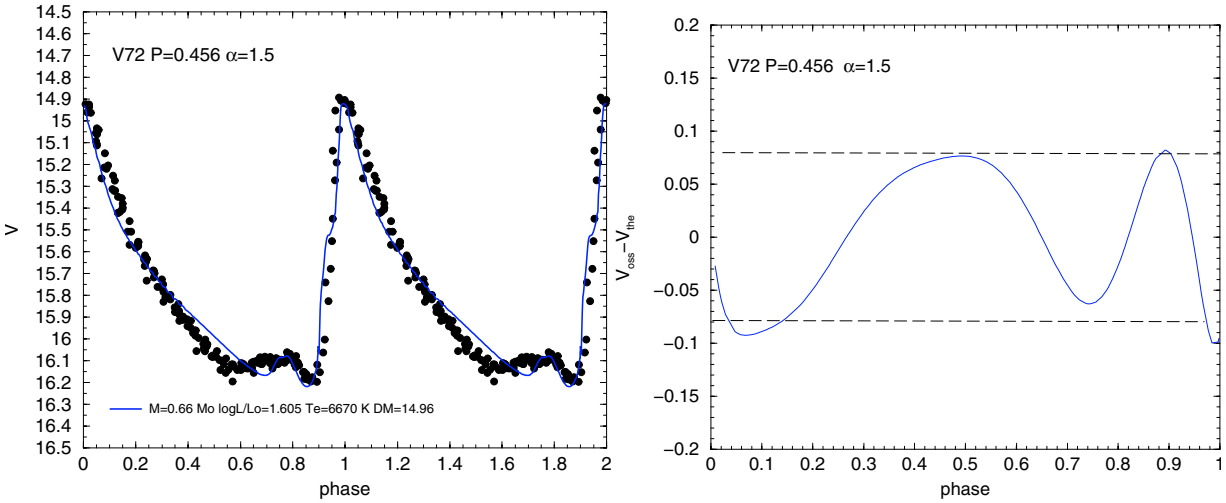

Fig. 12. The best match for the V72 light curve by adopting models with $\alpha = 1.5$. The *right panel* shows the residuals.

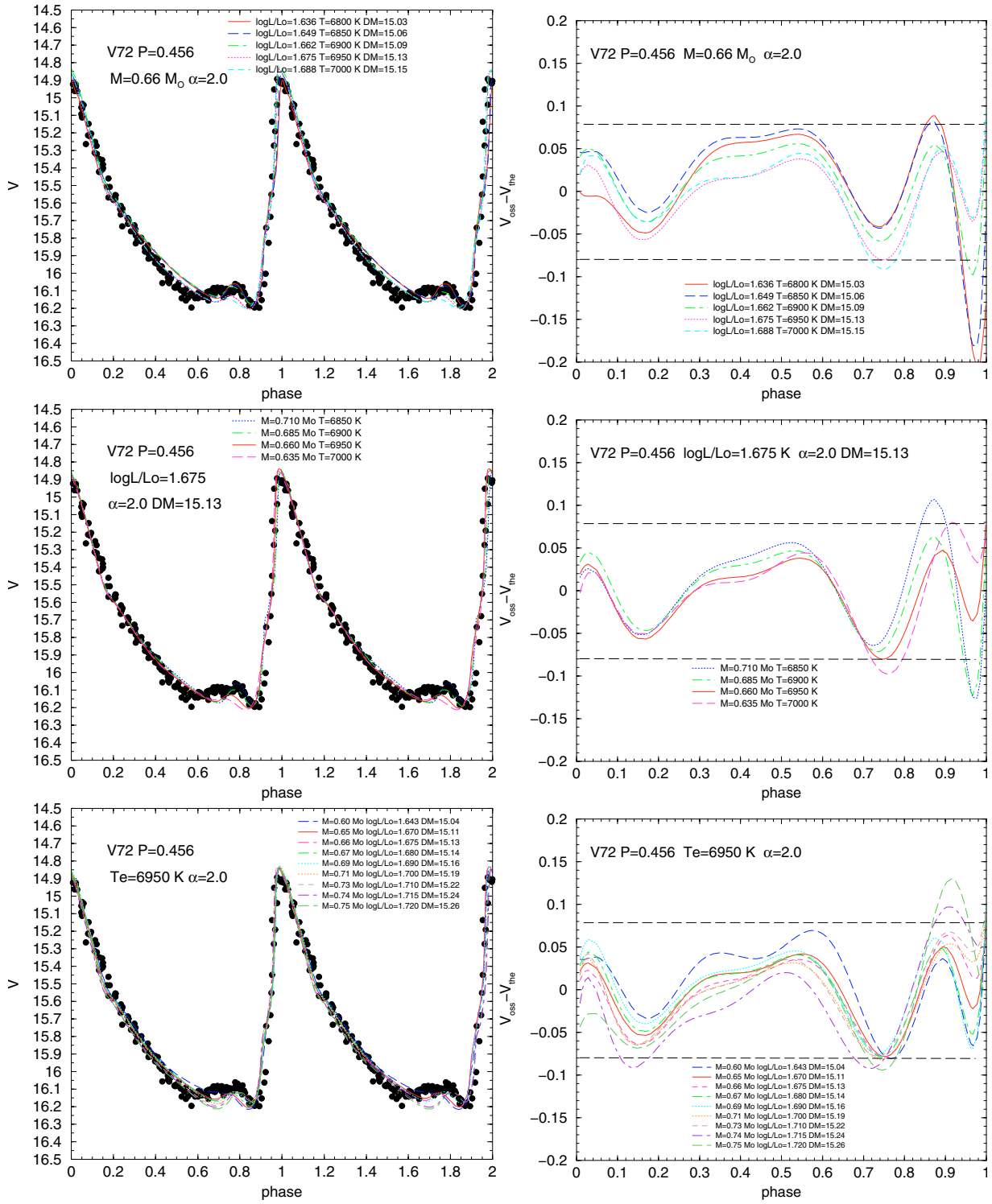

Fig. 13. Dependence of the modeling of V72 light curve on the input parameters, by fixing them one at a time (see text). *Upper panels*: fixed mass; *middle panels*: fixed luminosity level; *lower panels*: fixed effective temperature.

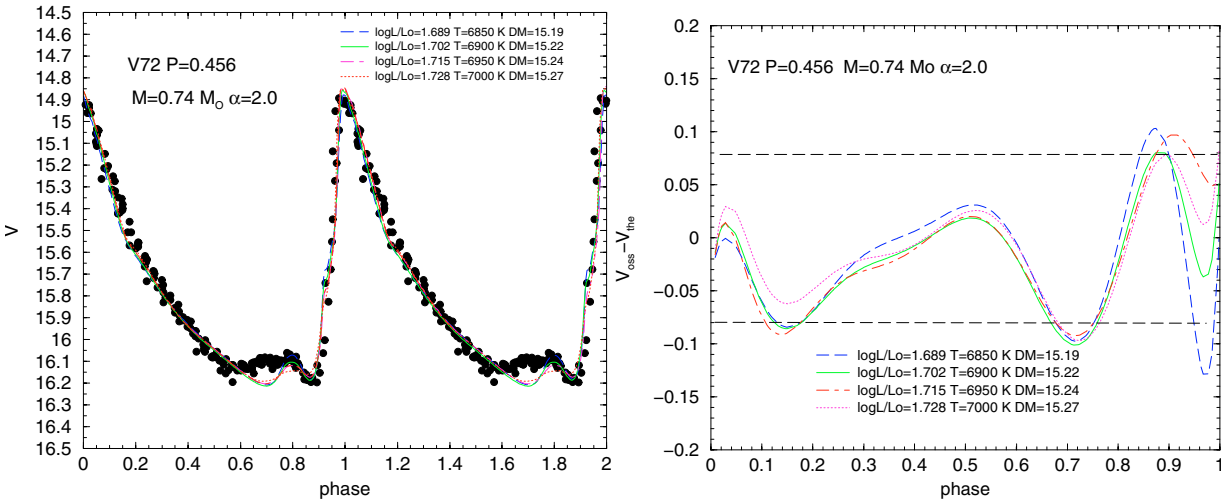

Fig. 14. Comparison between the data and the predicted light curves for $M = 0.74 M_{\odot}$ constrained to the observed period of V72.

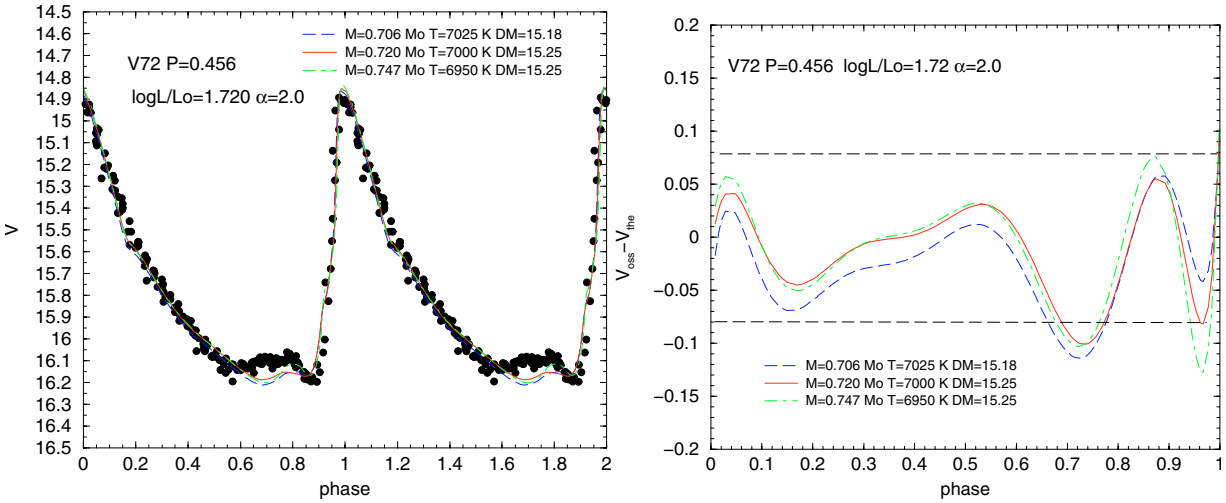

Fig. 15. Comparison between the data and the predicted light curves for V72 with fixed luminosity (log $L/Lo = 1.720$), see text.

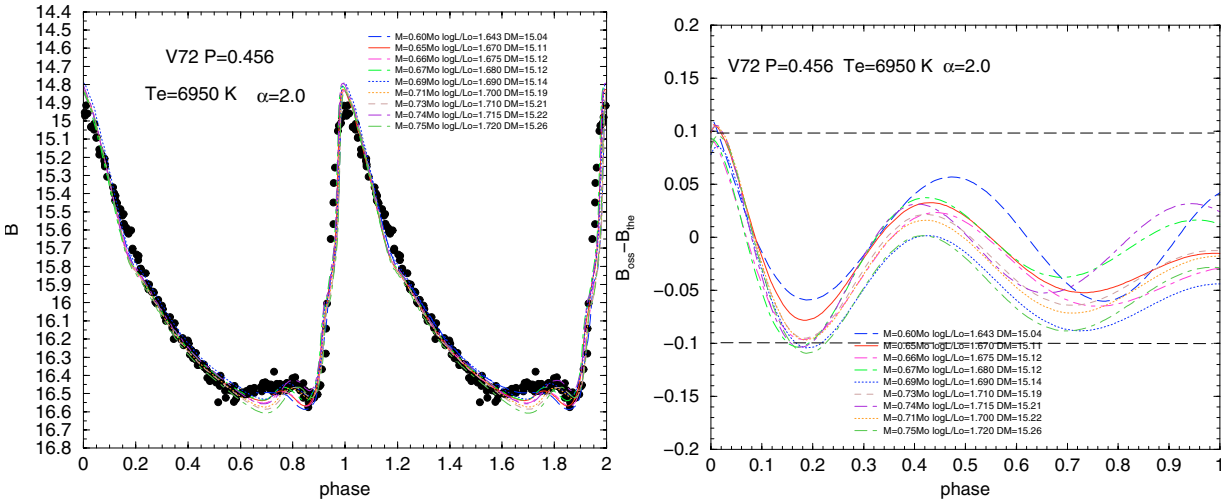

Fig. 16. As in the *bottom panels* of Fig. 13 but for the *B* band.

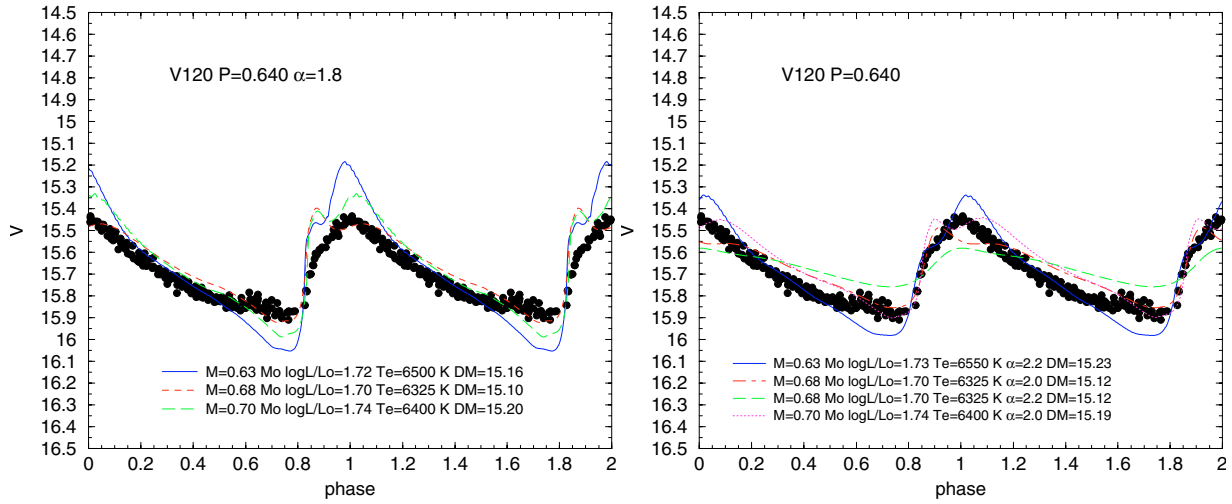

Fig. 17. Attempts of modeling the V120 light curve when α is fixed at 1.8 (*left panel*) or allowed to vary (*right panel*), see text.

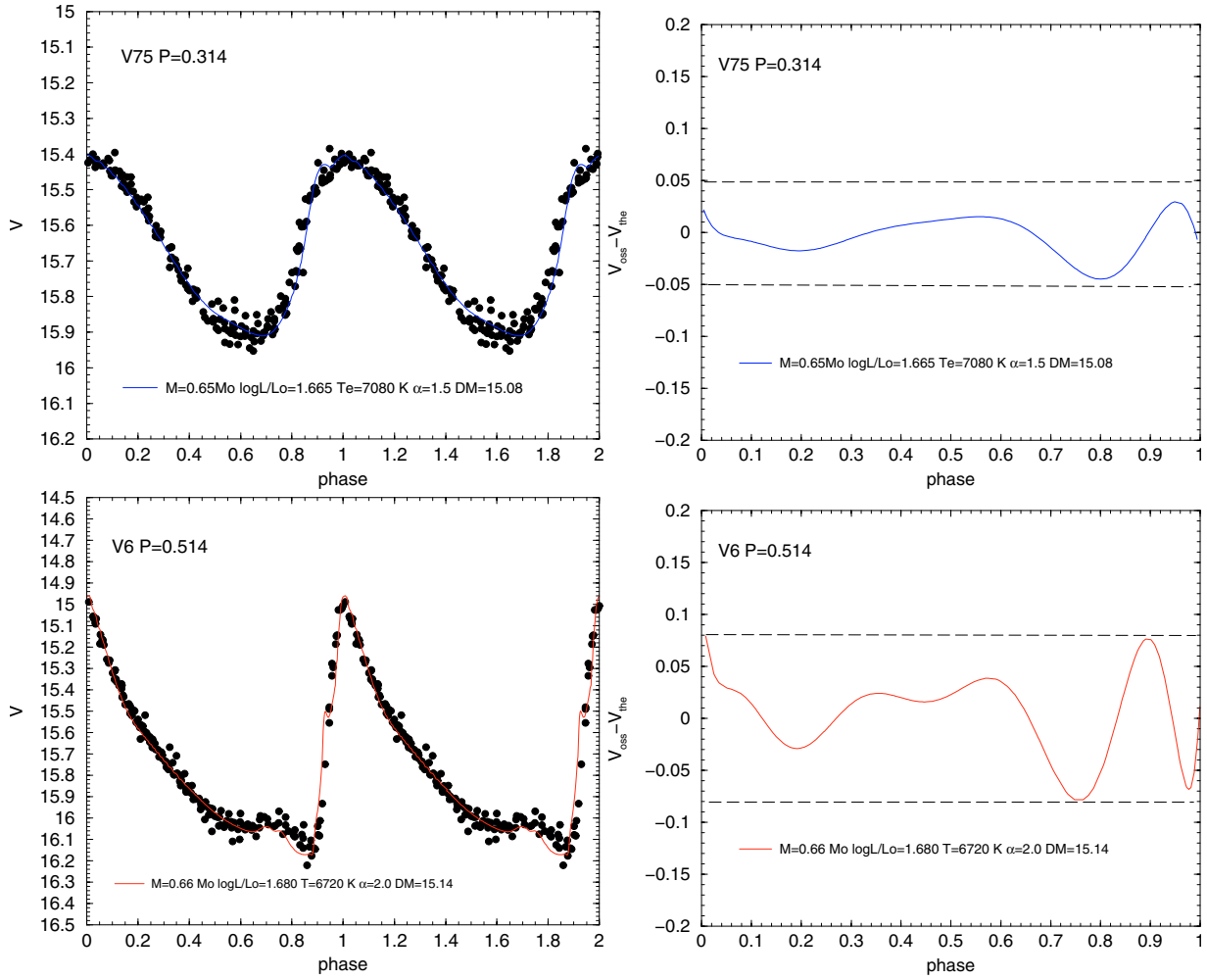

Fig. 18. Observed light curves in the *V* band for the V75 and V6 variables from CC01, compared with one of the possible theoretical matches. The periods (in days), the physical parameters of the selected models and the corresponding distance moduli are labeled.

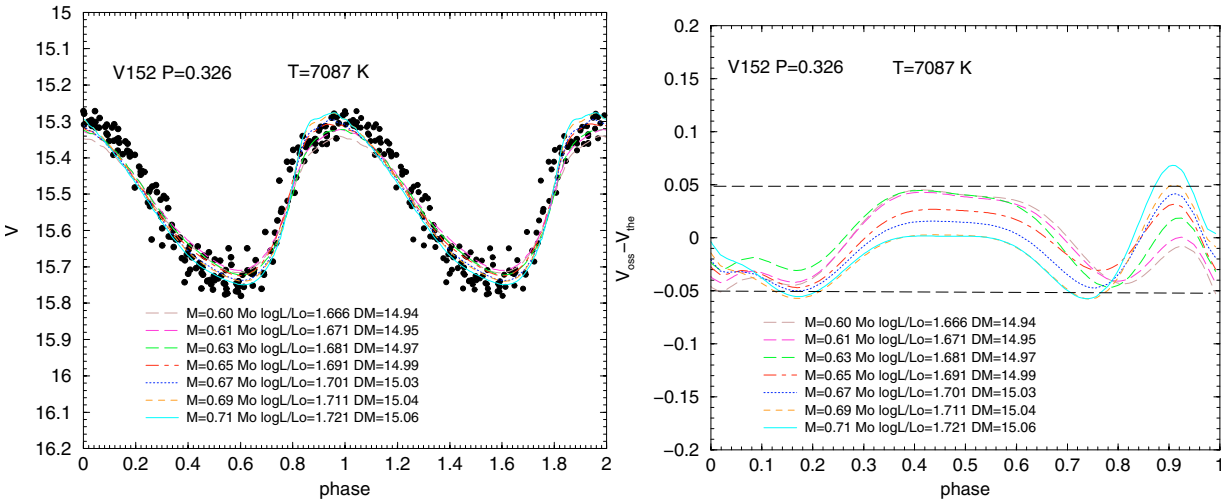

Fig. 19. Models at fixed effective temperature constrained to reproduce the observed V152 period compared with the observed data.

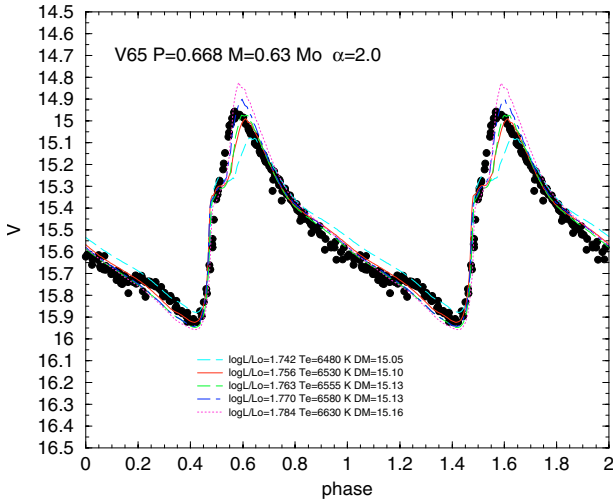

Fig. 20. Models for V152 with $M = 0.71\ M_{\odot}$ compared with the data.

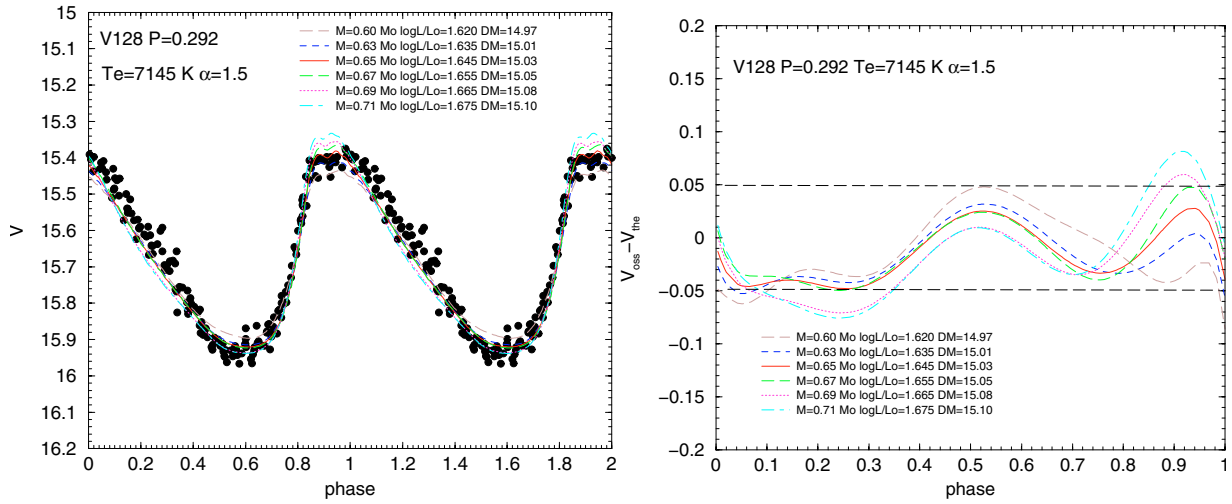

Fig. 21. As in the bottom panel of Fig. 2 but for $Z = 0.0004$ and a suitable value of the effective temperature (see text).

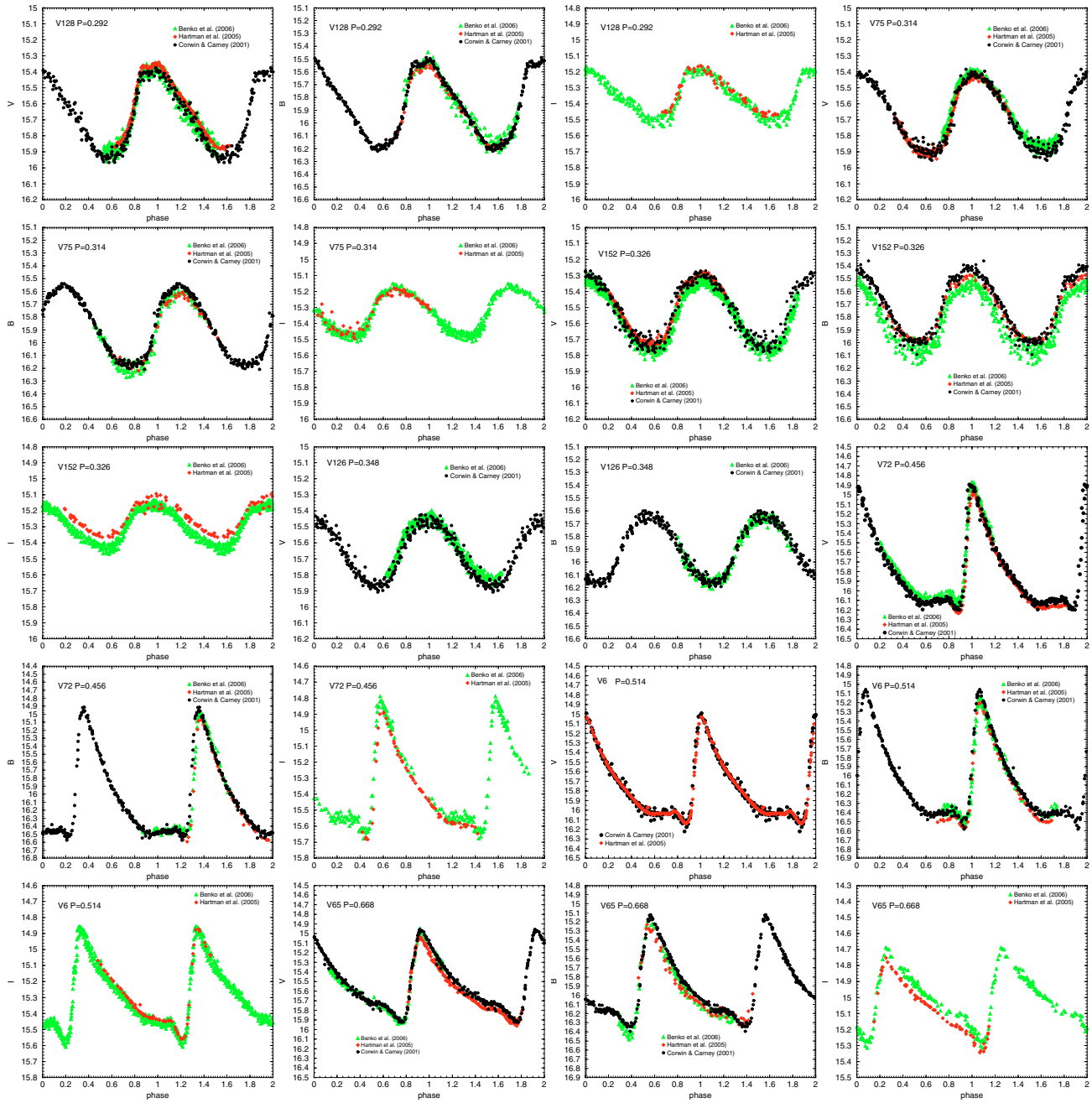

Fig. 22. Comparison (in the *V*, *B* and *I* bands) of the observed light curves analyzed in this paper by CC01 (black circles) with those of Hartmann et al. (2005) (red diamonds) and Benkő et al. (2006) (green triangles).

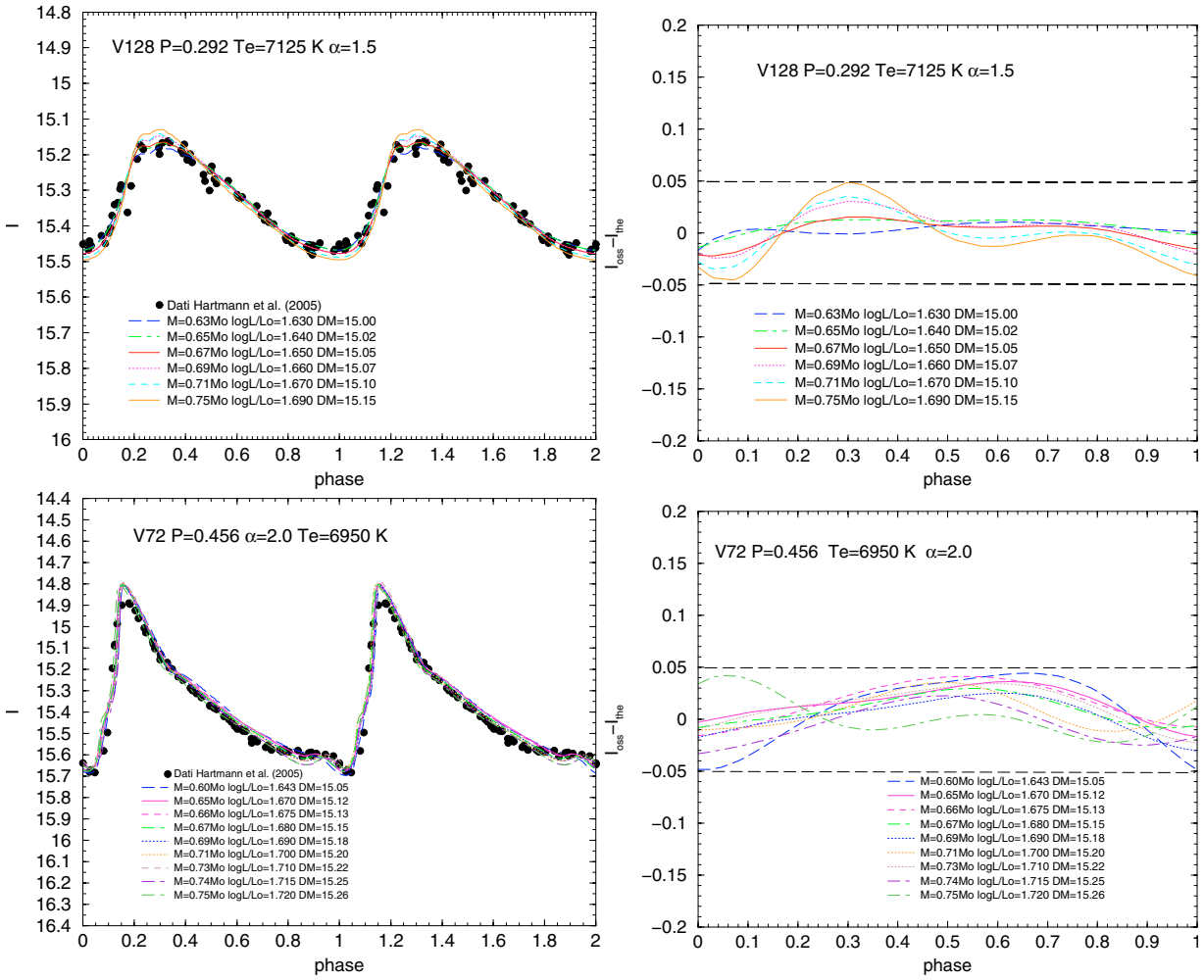

Fig. 23. *Upper panel*: the models of the *bottom panel* of Fig. 2 for V128 compared with the data by Hartmann et al. (2005) in the *I* band. *Lower Panel*: as in the upper panel but for the models in the *bottom panel* Fig. 13 for V72.